A Novel Missense Mutation in the SH2 Domain of the *STAT5B* Gene Results in a Transcriptionally Inactive STAT5b Associated with Severe IGF-I Deficiency, Immune Dysfunction, and Lack of Pulmonary Disease

Paula A. Scaglia,* Alicia S. Martínez,* Eva Feigerlová,* Liliana Bezrodnik, María Isabel Gaillard, Daniela Di Giovanni, María Gabriela Ballerini, Héctor G. Jasper, Juan J. Heinrich, Peng Fang, Horacio M. Domené, Ron G. Rosenfeld, and Vivian Hwa

Centro de Investigaciones Endocrinológicas (Consejo Nacional de Investigaciones Científicas y Técnicas) (P.A.S., A.S.M., M.G.B., H.G.J., J.J.H., H.M.D.) and Division of Endocrinology and Immunology Group (L.B., M.I.G., D.D.G.), "Ricardo Gutiérrez" Children's Hospital, 1330 Buenos Aires, Argentina; and Department of Pediatrics (E.F. P.F., R.G.R., V.H.), Oregon Health and Science University, Portland, Oregon 97239

Context: Signal transducer and activator of transcription 5b (STAT5b) deficiency, first reported in a patient who carried a p.Ala630Pro missense mutation in the Src homology 2 (SH2) domain, results in a rare clinical condition of GH insensitivity (GHI), IGF-I deficiency (IGFD), and severe immune dysregulation manifesting as progressive worsening of pulmonary function.

Patient: The new patient presented with severe cutaneous eczema, episodic infections in the first years of life, and autoimmune thyroiditis. Immunological evaluation revealed T lymphopenia, but severe pulmonary symptoms were notably absent. She concomitantly exhibited pronounced growth failure, reaching an adult height of 124.7 cm [−5.90 SD score (SDS)]. Endocrine evaluations (normal provocative GH tests; low serum IGF-I, −3.7 SDS, and IGF-binding protein-3, −4.5 SDS) were consistent with GHI and IGFD.

Results: Analysis of the *STAT5B* gene revealed a novel homozygous missense mutation, p.Phe646Ser, located within the βD′ strand of the SH2 domain. Reconstitution studies demonstrated expression of the p.Phe646Ser variant was less robust than wild type but, in contrast to the previously described *STAT5B* p.Ala630Pro SH2 mutation, could be phosphorylated in response to GH and interferon-γ. The phosphorylated p.Phe646Ser, however, could not drive transcription.

Conclusion: A novel *STAT5B* p.Phe646Ser mutation has been identified in a patient with clinical characteristics of STAT5b deficiency. Only the second *STAT5B* missense mutation identified, its lack of transcriptional activities despite GH-induced phosphorylation, confirms the crucial role of STAT5b for regulating the expression of *IGF1* and provides insights into the importance of the SH2 βD′ strand for full STAT5b transcriptional activities. Whether the phosphorylated p.Phe646Ser variant retained functions that prevented pulmonary distress remains unresolved. **(*J Clin Endocrinol Metab* 97: 0000–0000, 2012)**

ISSN Print 0021-972X ISSN Online 1945-7197
Printed in U.S.A.

doi: 10.1210/jc.2011-2554 Received September 13, 2011. Accepted February 2, 2012.

* P.A.S., A.S.M., and E.F. contributed equally to this work.

Abbreviations: FOXP3, Forkhead box P3; GHBP, GH-binding protein; GHI, GH insensitivity; GHR, GH receptor; IFN, interferon; IGFBP, IGF-binding protein; IP, immunoprecipitation; JAK, Janus tyrosine kinase; LIP, lymphocytic interstitial pneumonia; NK, natural killer; PBMC, peripheral blood mononuclear cells; PHA, phytohemagglutinin; pY, phosphorylated tyrosine; SDS, SD score; SH2, Src homology 2; STAT5b, signal transducer and activator of transcription 5b; TCR, T cell receptor; Treg, T lymphocyte regulatory.

Growth hormone insensitivity (GHI) is characterized by severe postnatal growth retardation, low IGF-I, and normal to elevated GH serum levels. The first cases described by Laron *et al.* (1) were later demonstrated to be linked to molecular defects in the GH receptor gene (*GHR*) (2). More recently, specific defects downstream of the GHR have been identified (3). To date, the only signaling molecule to be directly implicated with severe GHI phenotype is the signal transducer and activator of transcription 5b (STAT5b). Because the first report in 2003 of a patient with a homozygous missense mutation, p.Ala630Pro (p.A630P), in the *STAT5B* gene by Kofoed *et al.* (4), only seven other STAT5b-deficient patients have been formally described (5–9), carrying nonsense or frameshift mutations within the *STAT5B* gene, all of which are expected to result in the absence of functional STAT5b protein.

The human *STAT5B* gene, located at chromosome 17q11.2, contains 19 exons encoding a protein of 787 amino acids that consists of several domains: the amino-terminal, the coiled-coil, the DNA-binding, the linker, the Src homology 2 (SH2), and the transactivation domains. The STAT5b protein is a member of the STAT family of transcription factors (STAT1, -2, -3, -4, -5a, -5b, and -6) that are activated by hormones (*e.g.* GH and prolactin) and cytokines (*e.g.* interferon (IFN)-γ, IL-2, and IL-7). Extracellular binding of cytokines or GH to their specific receptors triggers the activation of receptor-associated Janus tyrosine kinases (JAK), which phosphorylates intracellular tyrosines on the receptors. Signaling molecules possessing SH2 domains, including STAT5b, are capable of binding these phosphotyrosine residues and become themselves tyrosine phosphorylated by the JAK. In the GH-GHR system, JAK2-mediated phosphorylation of STAT5b at Tyr699 results in STAT5b dimer formation through reciprocal Tyr699 binding via their SH2 domains. The STAT5b dimers then translocate to the cell nucleus where they act as transcription factors by binding to poorly characterized GH response elements in the promoter region of responsive genes and interact with coactivating proteins to stimulate transcription of genes such as *IGF1*, *IGFALS*, and *IGFBP3*.

We previously reported the first STAT5b-deficient patient, who carried the homozygous missense mutation p.A630P, located within the highly conserved SH2 domain (4). This case presented with GHI associated with immune dysregulation and severe autoimmune pulmonary disease (10). An update of the pulmonary disease progression in this first case (patient 1 in *Case reports*) is provided. We now describe a new case (patient 2), who carries only the second homozygous missense mutation identified in the *STAT5B* gene, also located in the SH2 domain. Functional studies and clinical presentation of the novel mutation, compared with p.A630P, revealed some striking differences and provided valuable insights as to possible phenotype-genotype correlations. Importantly, this mutation results in a protein capable of phosphorylation but incapable of transcriptionally activating *IGF1*.

Patients and Methods

Case reports

Patient 1

The history of growth and endocrine abnormalities of this patient, who carries a homozygous *STAT5B* missense mutation, p.A630P, was previously reported (4). Immunological evaluation had indicated that T lymphocyte regulatory (Treg) cells ($CD4^+FOXP3^+CD25^{high}$) were abnormally low due to dysregulation of the transcription factor forkhead box P3 (FOXP3) (10).

The female subject, born to consanguineous parents in Argentina, presented with chronic pulmonary distress, in addition to growth failure, from infancy. A particularly severe episode of respiratory disease at age 7 yr failed to respond to empiric antibiotic treatment. A lung biopsy showed infiltration of the interstitial spaces with lymphocytes (Fig. 1A), consistent with lymphocytic interstitial pneumonia (LIP), a condition associated with autoimmunity. Despite combined immunosuppressive therapy (prednisone and azathioprine), progressive worsening of pulmonary function (requiring mechanical ventilation), hemorrhagic varicella, and recurrent viral infections occurred by age 10 yr. Computed chest tomography showed worsening LIP, with signs of fibrosis (Fig. 1B), and a biopsy

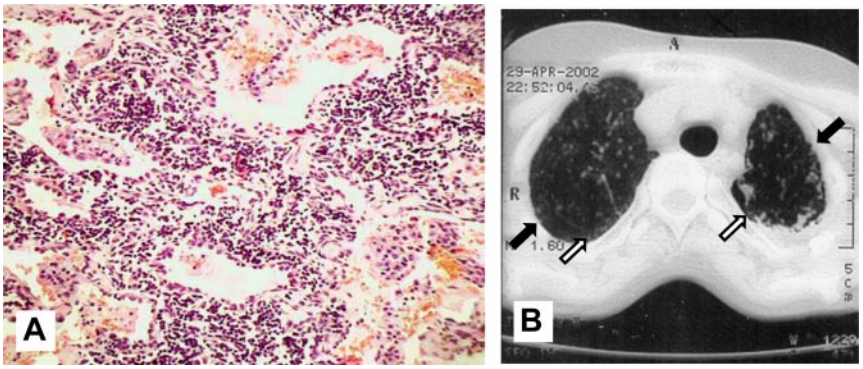

FIG. 1. A, Histological analysis of lung tissue from patient 1 at 7 yr of age demonstrating features of LIP. The fragment of lung parenchyma measured 2.5 × 1.5 × 0.3 cm. Although there is relative preservation of histological architecture, there is a marked and diffuse interstitial mononuclear cellular infiltrate with a follicular pattern that broadens the alveolar septa but largely spares the alveolar spaces. The peribronchial areas are also involved with this cellular infiltrate. B, Axial chest computerized tomography scan of patient 1 showing centrilobular nodules (*white arrows*) and subpleural nodules (*black arrows*).

indicated the presence of *Pneumocystis carinii*. Treatment with trimethoprim-sulfamethoxazole improved pulmonary function and was continued as prophylaxis, along with cyclosporin A. The patient, at age 23 yr, was awaiting a lung transplantation because this procedure has successfully alleviated the debilitating symptoms associated with pulmonary immune disease in one STAT5b-deficient subject (9).

Patient 2

The new female patient, born in Argentina (birth weight 2250 g, birth length 44 cm), was adopted at 4 d of age. Data regarding family and perinatal history are not available. Karyotype was 46,XX. She had an adequate weight gain until the third month of age, when the onset of episodic infections led to failure to thrive. At age 1 yr, she developed severe generalized seborrheic dermatitis, which persisted for several years. Autoimmune thyroiditis (positive anti-thyroid peroxidase and anti-thyroglobulin antibodies, 476 and 267 IU/ml, respectively) was diagnosed at 4.5 yr, and she was started on L-T_4 therapy. In later years, she developed severe varicella with cutaneous infection and *Streptococcus pyogenes* septicemia. It was of note that compromised pulmonary function was not observed throughout childhood or adolescence.

The patient concomitantly presented with severe postnatal growth retardation. At age 2.1 yr, she had a height of 67 cm, a weight of 6.2 kg [−6.0 and −4.5 SD score (SDS), respectively] (11), a head circumference of 43.5 cm (below third centile), a bird facies with micrognathia, frontal bossing, and synophrys. Psychomotor and neurological development was mildly delayed. At 11.2 yr, she was prepubertal, with a height of 106.8 cm (−4.30 SDS), weight 16.0 kg (−3.65 SDS), and bone age 10.0 yr (Fig. 2A). GH provocative tests were normal, with extremely low serum IGF-I and IGF-binding protein (IGFBP)-3. She spontaneously started puberty at 12.5 yr, reaching normal menarche at 14.5 yr (12, 13). A low growth spurt, with peak height velocity of only 4.2 cm/yr (below third percentile; normal, 7.5 cm/yr for age 13.8 yr) was noted. Pubertal height gain was 12.2 cm (Fig. 2B). She had irregular menses, followed by more than 10 months of normogonadotropic amenorrhea, resuming regular cycles at age 18. Her final adult height was 124.7 cm (−5.90 SDS) with a weight of 27.0 kg (body mass index −0.97 SDS).

Methods

The study was conducted in accordance with the Helsinki Declaration. Written informed consent for molecular studies was obtained from the patient, the normal controls, and their parents.

Endocrinological evaluation

Serum IGFBP-3 was measured by immunoradiometric assay (Diagnostic Systems Laboratories Inc., Webster, TX), total IGF-I by an in-house RIA (14), and serum GH and prolactin by chemiluminescent immunometric assays (Immulite 2000; Siemens Healthcare Diagnostics, Llamberis, Gwynedd, UK). Macroprolactin was estimated by measuring prolactin before and after polyethylene glycol precipitation, as previously described (15). GH-binding protein (GHBP) was evaluated using a time-resolved in-house fluorometric immunofunctional assay as previously described (16).

For the IGF-I generation test, serum IGF-I and IGFBP-3 were measured before and after the administration of recombinant human GH (0.033 mg/kg · d) for 7 d.

Immunological evaluation

Total serum Ig (IgG, IgM, and IgA) were measured by nephelometry using commercially available kits (Array 360; Beckman

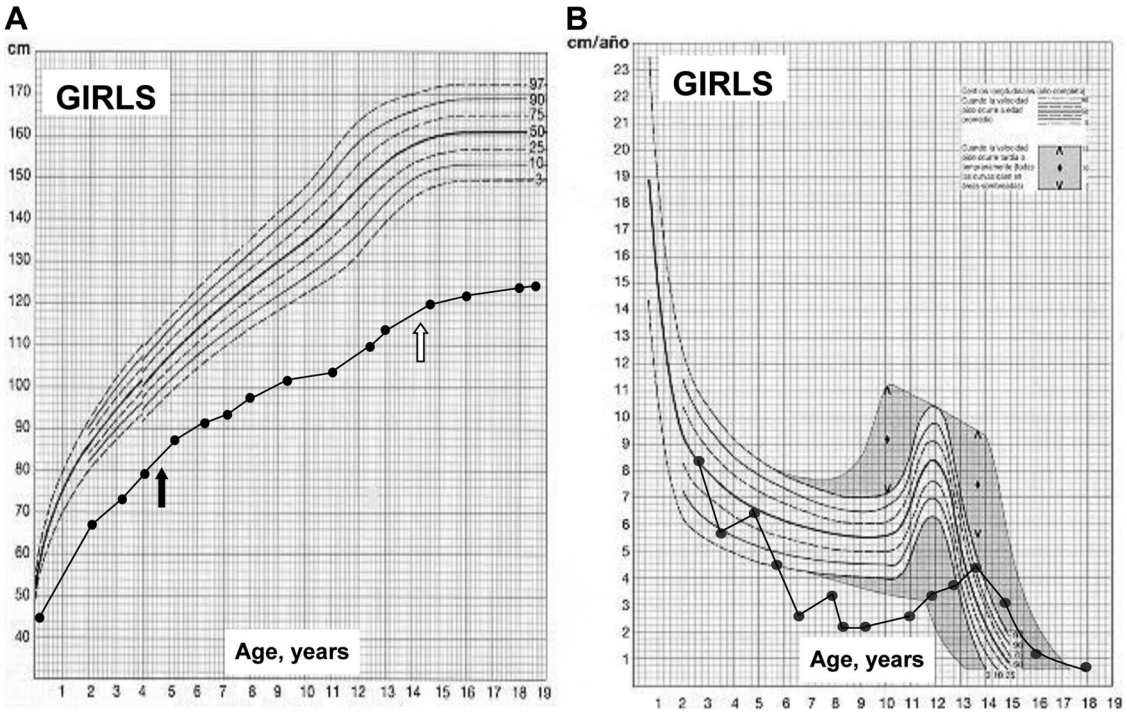

FIG. 2. Growth chart for height (A) and growth velocity (B) of patient 2. The *black arrow* indicates the onset of L-T_4 treatment and the *white arrow* the age of menarche.

Coulter Inc., Fullerton, CA) and IgE by microparticle enzyme immunoassay (Abbott Diagnostics, Buenos Aires, Argentina).

Peripheral cell subsets CD3, T cell receptor (TCR) $\alpha\beta$, TCR$\gamma\delta$, CD4, CD4CD45RA (naive), CD4CD45RO (memory), CD8, CD19, natural killer (NK) ($CD3^{-}CD16^{+}CD56^{+}$) were determined from fresh whole blood by FACSCalibur flow cytometry (Becton Dickinson, San Jose, CA). Treg cells ($CD4^{+}FOXP3^{+}CD25^{high}$) were determined on peripheral blood mononuclear cells (PBMC) by flow cytometry.

Proliferative responses of PBMC to phytohemagglutinin (PHA), PHA plus recombinant IL-2, anti-CD3 (Becton Dickinson, San Jose, CA), and phorbol myristate acetate plus ionomycin (Sigma-Aldrich, St. Louis, MO) were measured by [^{3}H]thymidine incorporation.

NK-cell activity was evaluated by flow cytometry with 1×10^6/ml K562 cells (a human erythroleukemia cell line) as target. PBMC effector cells from patient 2 were isolated by centrifugation with Ficoll-Hypaque and resuspended to a final concentration of 5×10^6 cells/ml. Different concentrations of effector cells were added to target cells and the mixture incubated for 4 h at 37 C under 5% CO_2 with propidium iodine (Sigma-Aldrich). Analyses were performed using CellQuest software (Becton Dickinson). The values of different subpopulations and functional studies were compared with our reference population.

Molecular studies

Genomic DNA from the patient and the normal controls was extracted from venous peripheral blood employing a cetyltrimethylammonium bromide lysis buffer and isoamyl alcohol-chloroform extraction method (17). The whole coding sequence (exons 2–19) and intron-exon boundaries corresponding to *STAT5B* gene (GeneID 6777, NG_007271.1, NM_012448.3, and NP_036580.2) were PCR amplified from genomic DNA and sequenced (Applied Biosystems 3730xl DNA analyzer; Macrogen Inc., Seoul, Korea). Oligonucleotide primers used are available upon request. The DNA samples of 50 Argentinean healthy subjects were used as controls.

Generation of recombinant mutant N-FLAG-STAT5b plasmids

N-terminally FLAG-tagged wild-type STAT5b (F-STAT5b) and FLAG-STAT5b-A630P (F-A630P) were previously described (18). F-STAT5b-F646S (F-F646S) was generated by site-specific mutagenesis (QuikChange II Site-Directed Mutagenesis Kit; Stratagene, La Jolla, CA), using F-STAT5b as template. The primers used were forward 5′-aatctgatgccttctaccaccagagacttctcc-3′ and reverse 5′-ggagaagtctctggtggtagaaggcatcagatt-3′. The nucleotide substitutions are *underlined*.

Cell culture and transfection experiments

HEK293 cells stably transfected with the full-length human *GHR* cDNA, HEK293(hGHR) (19), were maintained in DMEM (Cellgrow; Mediatech, Herndon, VA) supplemented with 10% fetal bovine serum (Invitrogen Life Technologies Inc., Grand Island, NY) at 37 C in 5% CO_2. To maintain selection, 400 μg/ml G418 (Sigma-Aldrich) was added to the culture medium. For reconstitution studies, HEK293(hGHR) cells were seeded at 2×10^5/well, grown to approximately 60% confluence in six-well tissue culture plates, and transiently transfected with 1 μg vector, pcDNA3.1, or 1 μg vector carrying F-STAT5b, F-F646S, or F-A630P using TransIT-LT1 (Mirus, Madison, WI). After 24 h transfection, cells were washed and serum starved for 9 h before a 20-min treatment with 100 ng/ml recombinant human GH (generous gift from Merck-Serono, Buenos Aires, Argentina) or 100 U/ml IFN-γ (Roche, Mannheim, Germany), as described previously (18). Transfection experiments were performed in duplicates, at least three independent times.

Luciferase reporter assay

The luciferase reporter construct carrying 8xGH response element (GHRE) from the rat Spi2.1 gene in pGL2 (pGHRE-LUC) was a generous gift from Drs. Woelfle and Rotwein (Oregon Health and Science University, Portland, OR).

HEK293(hGHR) cells were seeded as described above, and transfected with a total of 2 μg input DNA per well: 1 μg pGHRE-LUC plus 1 μg pcDNA3.1 or relevant F-STAT5b variants (F-STAT5b, F-F646S, or F-A630P). After treatment with GH or IFN-γ for 18–24 h, collected cell lysates were analyzed for reporter activity using the luciferase assay system (Promega Corp., Madison, WI) following the manufacturer's protocol. Luciferase activities were measured with a luminometer (BioTek Instruments Inc., Winooski, VT). The total amount of cell lysates analyzed is as indicated. The results are reported as relative fold induction ± SD, compared with activities detected in 20 μg total protein of untreated, pcDNA3.1-transfected cell lysates, which was given an arbitrary unit value of 1. Calculated values were from at least two independent experiments, performed in duplicate.

Antibodies

Antibodies against phospho-tyrosine-STAT5 were obtained from Cell Signaling Technology (Beverly, MA); anti-STAT5b (G2) from Santa Cruz Biotechnology, Inc. (Santa Cruz, CA); anti-FLAG M2 antibody, anti-FLAG-M2-agarose gel [for immunoprecipitation (IP)] from Sigma; and secondary antibodies antimouse IgG and antirabbit IgG from Amersham-Pharmacia Biotech (Uppsala, Sweden).

IP and Western immunoblot analysis

Cell lysates were solubilized in Triton X-100 lysis buffer as previously described (18). Total cell lysates (150–300 μg) were IP using anti-FLAG-M2-agarose affinity gel, size fractionated on reducing 7% SDS-PAGE gels, and electroblotted onto nitrocellulose membranes. Western blots were processed with the appropriate primary and secondary antibodies, following the manufacturers' protocols, and visualized by enhanced chemiluminescence (PerkinElmer Life Sciences Inc., Boston, MA).

Results

Clinical phenotype of patient 2 is consistent with a STAT5b deficiency

The severe growth failure observed in patient 2 was associated with normal GH provocative tests, abnormally low serum IGF-I and IGFBP-3 (Table 1), and nonresponsiveness to an IGF-I generation test (Table 2). GHBP levels were normal (Table 1). These observations are consistent with GHI. Unlike GHI patients, however, serum prolactin was markedly elevated (83 ng/ml; reference values, <25

TABLE 1. Hormonal evaluation of patient 2

	Patient 2	Reference values
GH (μg/liter)		
Basal	1.7	
Peak after arginine (30 min)	13.3	>6.0
Peak after clonidine (90 min)	27.1	>6.0
IGF-I (μg/liter)	16	119–483
IGFBP-3 (mg/liter)	0.84	2.1–7.4
GHBP (nmol/liter)	1.2	1.0–6.2
Prolactin (μg/liter)	83	3–25

ng/ml) but was not due to macroprolactinemia, because macroprolactin was undetectable. Episodic infections, severe dermatitis, and autoimmune thyroiditis, furthermore, were consistent with immune dysfunction. Unlike patient 1 (see *Case reports*); however, pulmonary symptoms were notably absent.

Immunological evaluation indicated IgG and IgA hyper-γ-globulinemia (Table 3). $CD19^+$ cells were normal, whereas $CD3^+$ T lymphocytes were significantly decreased with abnormalities in the proportion of $CD3^+$ cells carrying TCRαβ or TCRγδ. Absolute counts of $CD4^+$ and $CD8^+$ cells were significantly below normal (Table 3), with markedly low relative counts of $CD8^+$. Analysis of the $CD4^+$ subpopulation revealed low percentages of naive CD4CD45RA cells and high percentages of activated CD4CD45RO cells. Furthermore, $CD4^+FOXP3^+CD25^{high}$ cells were reduced. *In vitro* T cell proliferation responses to PHA (40×10^3 counts/min; reference values, $62–160 \times 10^3$ counts/min) and anti-CD3 (25×10^3 counts/min; reference values, $49–118 \times 10^3$) were low but restorable by addition of recombinant IL-2.

Absolute numbers of NK cells ($CD3^-CD16^+CD56^+$) were low, although NK activity was in the low-normal range: effector to target at a ratio of 50:1 generated a cytotoxicity of 15%, compared with the normal mean cytotoxicity of 30 ± 15%.

The complex clinical phenotype of GHI in association with high prolactin and immune dysregulation was strongly suggestive of a STAT5b deficiency.

TABLE 2. IGF-I generation test of patient 2 (performed at age 11.2 yr)

	IGF-I		IGFBP-3	
	μg/liter	SDS	mg/liter	SDS
Basal	ND		0.84	−4.5
d 5	12	−4.0	1.32	−4.1
d 8	11	−4.0	1.3	−4.1

ND, Not detectable.

TABLE 3. Immunological evaluation of patient 2

	Patient 2	Reference values
IgG (mg/dl)	2240	1264 ± 280
IgA (mg/dl)	452	182 ± 70
IgM (mg/dl)	158	151 ± 69
IgE (IU/ml)	28	<100
$CD3/mm^3$ (%)	540 (50%)	1400–2000
$CD4/mm^3$ (%)	432 (40%)	700–1100
$CD8/mm^3$ (%)	86 (8%)	600–900
$CD19/mm^3$ (%)	400 (37%)	300–500
NK ($CD3^-CD16^+CD56^+$)/mm^3 (%)	87 (8%)	148–332
TCRαβ (%)	95	54–66
TCRγδ (%)	2	5–8
CD4CD45RA (%)	7	65–73
CD4CD45RO (%)	91	39–57
Treg ($CD4^+FOXP3^+CD25^{high}$) (%)	1%	2–6%

Novel missense mutation identified within the SH2 domain of the *STAT5B* gene

Sequencing of the *STAT5B* gene in patient 2 revealed a T to C transition in exon 16, corresponding to the second nucleotide of codon 646 (*c.1937T→C*), which changed phenylalanine (Phe, F) to serine (Ser, S) (p.Phe646Ser; p.F646S) (Fig. 3). The results are consistent with either a homozygous or hemizygous state. No polymorphism or heterozygosity was detected at this position in 50 Argentinean control genomic DNA samples, nor was this variant reported in the NCBI dsSNP database (http://www.ncbi.nlm.nih.gov/projects/SNP/). *In silico* analysis (PolyPhen-2, http://genetics.bwh.harvard.edu/pph2/) predicted p.F646S mutation to be probably damaging, with a score of 0.991 (sensitivity, 0.60; specificity, 0.96). F646 lies within the SH2 domain in STAT5b and is highly conserved among all STAT5b proteins from multiple animal species.

GH-induced phosphorylation of recombinant F-F646S

Because primary cells from the patient were not available, we regenerated a recombinant N-terminally FLAG-tagged STAT5b p.F646S variant for reconstitution studies in HEK293(hGHR). The impact of the missense F646S substitution on STAT5b protein expression and function was evaluated and compared with wild-type F-STAT5b and to our previously described missense mutation, F-A630P (18). Equivalent amounts of HEK293(hGHR) cell lysates (200 μg total protein), transiently transfected with vector or one of the F-STAT5b variants, were IP with anti-FLAG and immunoblotted as indicated (Fig. 4A). Expression of F-F646S was consistently less than that of wild-type F-STAT5b but equivalent to that of F-A630P (Fig. 4A). When immunologically equivalent amounts of F-STAT5b variants were IP after GH treatment, phosphorylation of wild-type F-STAT5b (Fig. 4B) was robust, phosphorylation of F-A630P was poor, consistent with our previous results (20), but interestingly,

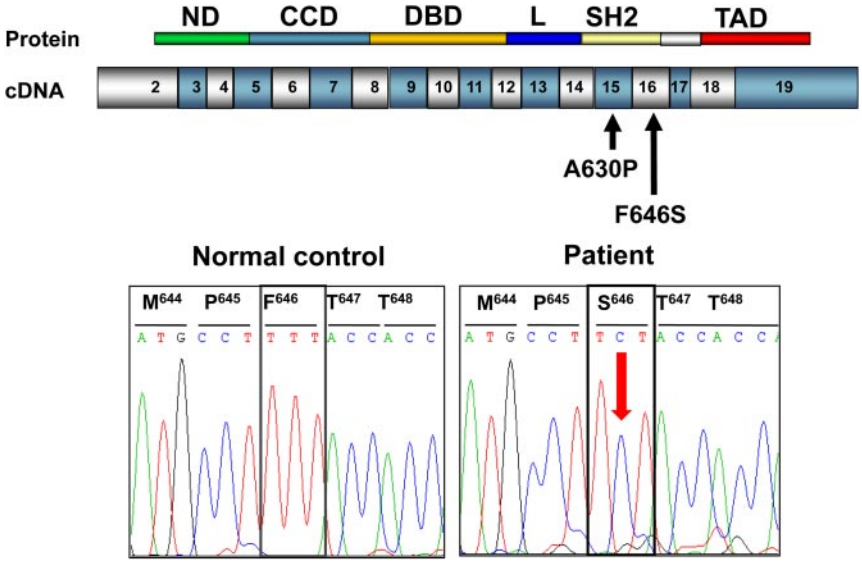

FIG. 3. Identification of the *STAT5B* p.Phe646Ser (p.F646S) mutation in patient 2. Schematic representation of *STAT5B* cDNA (exons as indicated) and protein, showing the localization of the present and previously described missense mutation, p.A630P, within the SH2 domain. Electropherograms show relevant DNA sequences from the *STAT5B* exon 16 in a normal control (wild-type sequence) and in the patient. CCD, Coiled-coil domain; DBD, DNA-binding domain; L, linker; ND, amino-terminal domain; TAD, transactivation domain.

GH-induced phosphorylation of F-F646S was distinctly and reproducibly detected, although phosphorylation was considerably less robust when compared with that of wild-type F-STAT5b.

Recombinant F-F646S cannot drive GHRE(Spi2.1) luciferase reporter activity

To determine whether the GH-induced phosphorylated F-F646S regulated gene transcription, an *in vitro* luciferase reporter assay system was employed. A basal 1.4-fold increase in luciferase activity was observed upon GH treatment in cells transfected with the vector (Fig. 4C). In cells transfected with wild-type F-STAT5b, luciferase activities were detected in 5 μg cell lysates (8.4-fold increase in activity), and activities increased 55.2-fold when 40 μg total cell lysates was tested (Fig. 4C). GH-induced reporter activity for 40 μg cell lysates expressing F-F646S protein, in contrast, was undetectable and similar to that of vector and F-A630P-transfected cells (Fig. 4C).

IFN-γ-induced phospho-tyrosyl F-F646S is transcriptionally inactive

Multiple growth factors and cytokines, including IFN-γ, can activate STAT5b by first recruiting STAT5b to the respective activated receptors. We determined whether other signaling systems such as IFN-γ, could, like GH, also activate F-F646S. Results showed that, similar to GH, IFN-γ can induce phosphorylation of F-F646S (Fig. 4D), but the phosphorylated STAT5b variant was unable to drive the luciferase reporter (Fig. 4E). As previously demonstrated, no phosphorylation or transcriptional activities were observed for IFN-γ-treated cells transiently transfected with the F-A630P variant (18, 20).

Discussion

We describe a new case of IGF deficiency, severe short stature, and immune dysfunction, due to a novel homozygous missense mutation in the *STAT5B* gene. This patient (patient 2) represents the third STAT5b-deficient patient from Argentina and only the ninth formally reported case. The identified *STAT5B* mutation, p.F646S, is of particular interest, because only one other missense *STAT5B* mutation (p.A630P) has been described to date (patient 1) (4). Although both missense mutations are located within the critical SH2 domain of the STAT5b protein, the impact of p.F646S was distinct from that of p.A630P and, together, have provided valuable insights into STAT5b functions. These differences may have contributed to the subtle pathophysiological differences between the two patients.

The SH2 domain functions predominantly by binding only phosphorylated tyrosine (pY) residues. Pathogenic mutations in SH2 domains frequently involve amino acid residues essential for specificity in binding pY or that are important for protein stability (21). All SH2 domains are structurally similar containing a core of ß-sheets flanked by α-helices, with the positively charged phosphate-binding pocket located within the core ß-sheets and the specificity for the pY motifs proposed to be governed, in part, by loops that link the various ß-sheets and α-helices (22). Based on the crystal structures of STAT1 and STAT3 (23–26), the ß-core of STAT SH2 domains consists only of the ßB, ßC, and ßD-ßD′ of the seven ß-sheets typically found in SH2 domains (Fig. 5A).

In the STAT5b peptide A630 is located within ßC (Fig. 5A), which forms part of the phosphate-binding pocket. F646 lies within the ßD-ßD′ region (Fig. 5A), which in STAT1 and STAT3, was shown to contribute to pY binding by interacting with residues C-terminal (positions +1 to +4) of the pY (25, 26). Interestingly, in hyper-IgE syndrome, several *STAT3* dominant-negative mutations have been identified in the ßD-ßD′region (27), including a p.M637V that resulted in loss of ligand-induced phosphorylation (28).

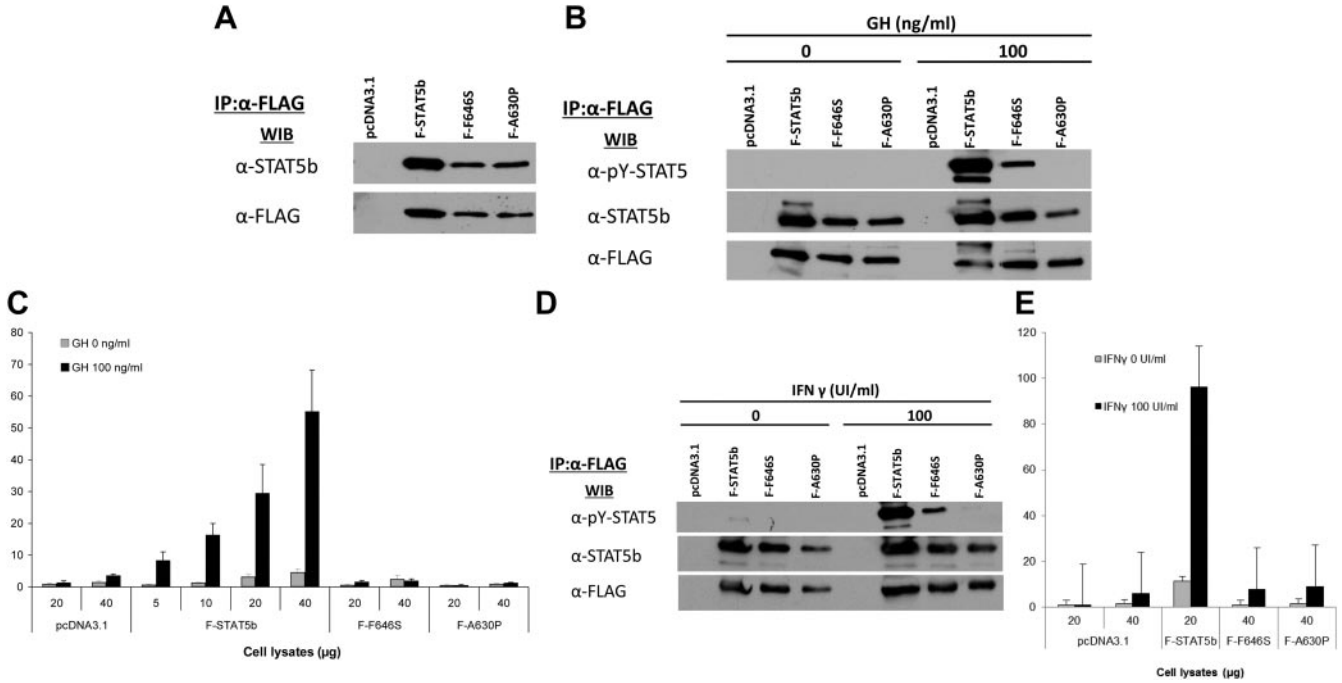

FIG. 4. STAT5B p.F646S can be activated by GH and IFN-γ in reconstitution experiments but is unable to drive luciferase activity. HEK293(hGHR) cells were transfected with plasmids pcDNA3.1, wild-type F-STAT5b, F-F646S, or F-A630P and treated with GH and IFN-γ for 20 min or as indicated. A, Cell lysates were collected and recombinant FLAG-tagged proteins were IP from 200 μg total protein before Western immunoblot (WIB) analysis. Antibodies used are indicated. B and D, Immunologically equivalent amounts of F-STAT5b variants were IP (F-F646S and F-A630P, each from 300 μg total cell lysates; and wild-type F-STAT5b from 150 μg total cell lysates), and responses to GH (B) and IFN-γ (D) treatments were evaluated. Immunoblots were stripped and reprobed with anti-STAT5b (*middle panel*) or anti-FLAG (*bottom panel*) antibodies. C and E, Cells cotransfected with pGHRE-LUC and F-STAT5b variant were treated with or without GH (C) or IFN-γ (E), and cell lysates were analyzed for luciferase activities. For cells cotransfected with wild-type F-STAT5b, increasing amounts of total cell lysates (5, 10, 20, and 40 μg) were tested. For the cells cotransfected with the F-STAT5b variants, 20 and 40 μg protein were analyzed. The results are reported as relative fold induction ± SD compared with untreated conditions (pcDNA3.1, 20 μg total protein) from at least two independent experiments, each performed in duplicates.

Although the role of STAT5b ßD-ßD′ in binding pY motifs remains to be fully elucidated, a substitution at 646 in ßD′, from phenylalanine, a nonpolar aromatic amino acid residue, to serine, a small aliphatic polar residue, would be predicted to be disruptive. However, in reconstitution studies, GH-induced phosphorylation of the STAT5b p.F646S variant, unlike p.A630P, was readily observed but was consistently less than that detected with wild-type STAT5b, even when GH treatment was increased from 100 to 500 ng/ml (data not shown). Similar observations were made when treated with IFN-γ. The implication is that STAT5b p.F646S had retained the ability to associate with critical pY motifs on the GHR (29) and IFN-γ receptors (30). The lower concentration of detectable phospho-p.F646S, however, suggests a decreased affinity for the pY motifs, although the F646S mutation could have created conformational changes that affected JAK2-mediated phosphorylation or increased vulnerability to dephosphorylation.

Although phosphorylation of p.F646S was detectable, the variant failed to drive transcription. This was not due simply to the reduced number of phosphorylated variant peptides, because transcriptional activities were detectable at comparable, or even lower, concentrations of phosphorylated wild-type F-STAT5b (Fig. 4C). Whether the F646S substitution induced a shorter transitory phosphorylated state, thereby affecting stable homodimer formation necessary for translocation to the nucleus and for binding DNA (23), or modulated uncharacterized structural determinants necessary for transcriptional activities remains to be elucidated.

The functional loss of STAT5b p.F646S as a transcription factor is consistent with the clinical presentation of severe IGF-I deficiency and GHI in patient 2. Previous studies employing primary dermal fibroblasts carrying STAT5b p.A630P had demonstrated that transcriptional regulation of *IGF1* expression by GH (4) and IFN-γ (18) was STAT5b dependent. Patient 2, together with these studies and all described cases of STAT5b deficiency to date, confirms the critical importance of STAT5b for mediating GH-induced regulation of *IGF1* expression.

The profound IGF-I deficiency resulted in severe growth retardation, with patient 2 reaching an adult height of −5.90 SDS. Interestingly, puberty was not delayed, unlike STAT5b-deficiency cases of applicable age (31), although the pubertal growth spurt was markedly below normal and could be due to the actions of sex steroids (32). Altogether, growth and endocrine character-

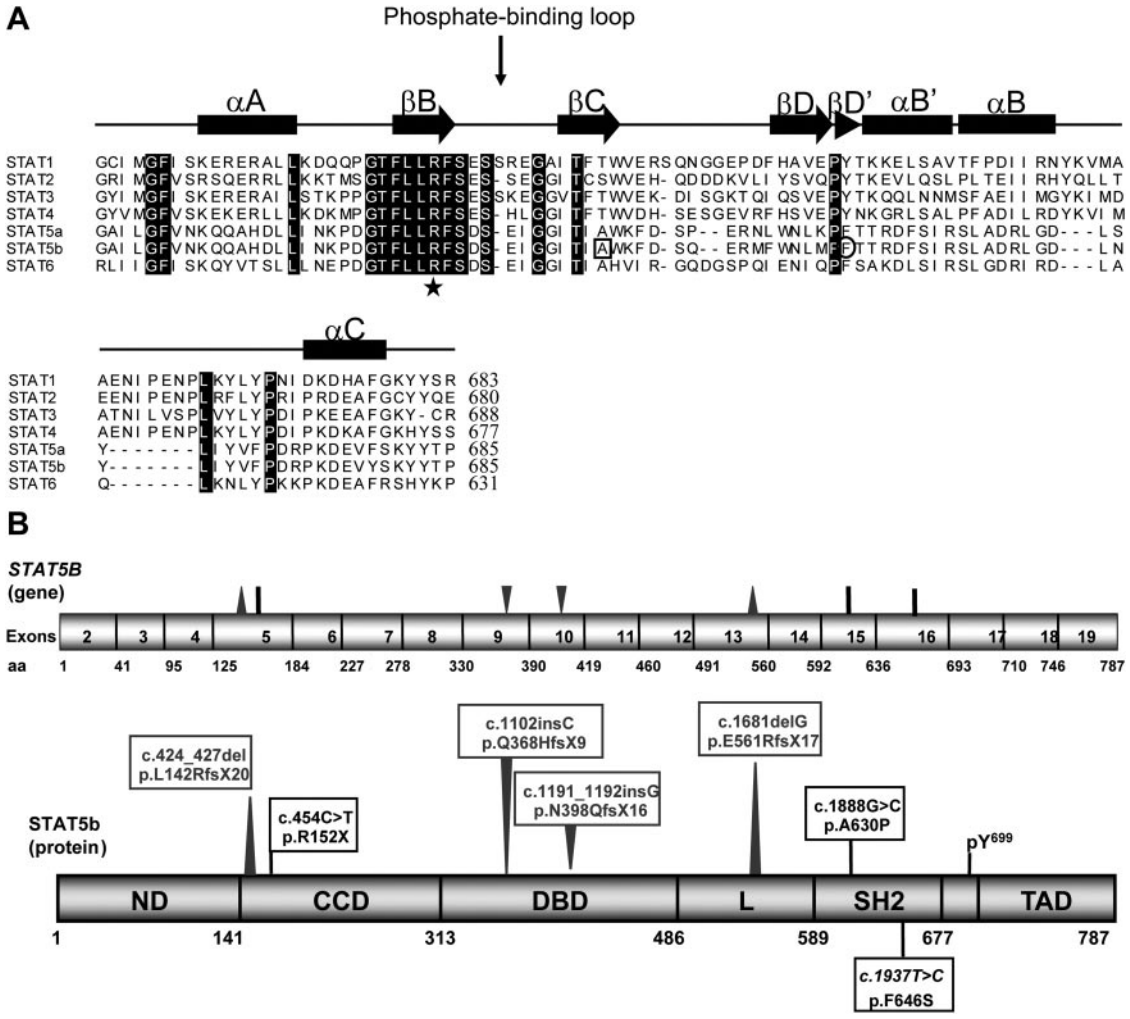

FIG. 5. Human *STAT5B* mutations. A, Sequence alignment and secondary structure of SH2 domains of human STAT proteins. The secondary structures, indicated above the sequence alignment, are based on a crystal structure of human STAT1 (23). The F646 residue, located within the βD′ region, is *circled*, and Ala at position 630, located in ßC, is *boxed*. The *asterisk* indicates the invariant Arg residue that specifically interacts with the phosphate group on pY. B, Schematic representation of the *STAT5B* cDNA and protein, showing locations of all previously described gene mutations (indicated above schematic of the STAT5b protein) with respect to the novel p.F646S mutation. CCD, Coiled-coil domain; DBD, DNA-binding domain; L, linker; ND, amino-terminal domain; TAD, transactivation domain.

istics were relatively indistinguishable among all described STAT5b-deficiency cases.

One striking difference between our two patients was the absence of pulmonary symptoms displayed by patient 2, despite a diagnosed T cell lymphopenia and other immune irregularities. For patient 1, pulmonary disease was severe, manifesting in early childhood, requiring corticosteroid therapy and mechanical intervention with oxygen treatment. The patient was awaiting a lung transplantation at age 23 (see *Case reports*). Indeed, a successful lung transplantation was reported to alleviate progressively impaired pulmonary functions in one STAT5b-deficient subject (9). Of the remaining STAT5b-deficient cases, two succumbed and died of progressive pulmonary fibrosis and respiratory failure (Berberoglu, M., personal communication, Miras M., personal communication) (5, 31). It was, therefore, of note that patient 2 lacked any of these severe and chronic pulmonary manifestations. Only one other STAT5b-deficient patient who was not severely immunocompromised has been described (7, 33). This adult male, in contrast to patient 2, had a normal immune profile (33) despite carrying a homozygous nucleotide insertion in the DNA-binding domain region (*c.1102insC*; Fig 5B) that would result in a predicted frameshift and truncation of the STAT5b protein. The mechanism for relative immune competency in this patient, however, remains a conundrum, because the majority of STAT5b-deficient subjects who suffer severe pulmonary distress carry nonsense or similar frameshift *STAT5B* mutations (Fig 5B) that could generate unstable mRNA expression or truncated STAT5b peptides.

The pulmonary diseases of patient 1 was attributed to abnormally low $CD4^+FOXP3^+CD25^{high}$ (Treg) cells as a consequence of the STAT5b p.A630P mutation (10), and

low Treg cells have been characterized in one other STAT5b-deficient case (6). In addition to the low Treg cells, severely low levels of CD8, low NK activity, and elevated activated $CD4^+CD45RO^+$ cells in patient 2 were similar to that reported for patient 1. Altogether, including presentations of persistent severe eczema and autoimmune thyroiditis, immune dysfunction was clearly indicated in patient 2. It is of note that in the reported STAT5b-deficient cases, other symptoms of immune irregularities include juvenile idiopathic arthritis (one subject) (8) and thrombocytopenic purpura (two subjects) (5, 9). For patient 2, it remains unclear why severe pulmonary disease was absent, despite indications of immune dysfunction and low Treg, but may be due, in part, to the presence of phosphorylated STAT5b p.F646S.

In summary, we have identified only the second homozygous *STAT5B* missense mutation, p.F646S, in a patient with profound postnatal growth failure due to IGF deficiency but who lacked the severe chronic pulmonary disease and immunodeficiency observed in the patient carrying the first described *STAT5B* missense mutation, p.A630P. Both missense mutations are located within the critical SH2 domain. Although the p.A630P substitution, mapping within the βC sheet, completely abrogated both the phosphopeptide binding and transcriptional functions, the p.F646S variant, located within the βD′ sheet, could still bind phosphopeptides but was unable to drive transcription, thus demonstrating the importance of the SH2 βD′ strand for full transcriptional activity. This differential functional effect of p.F646S is unique among the *STAT5B* mutations and may be correlated to the absence of pulmonary symptoms displayed by the patient. It is to be hoped that identification of additional STAT5b-deficient patients will result in more thorough genotype-phenotype correlations.

Acknowledgments

We thank Samantha Go for technical assistance with constructing F-F646S.

Address reprint requests to: Vivian Hwa, Ph.D., Department of Pediatrics, CDRC 2250, Oregon Health and Science University, 3181 SW Sam Jackson Park Road, Portland, Oregon 97239.

E.F. received support from the Fulbright Commission. This study was supported in part by a grant from the March of Dimes (to R.G.R.).

Disclosure Summary: P.A.S., A.S.M., L.B., M.I.G., D.D.G., H.M.D, M.G.B, H.G.J, J.J.H, E.F., P.F., R.G.R., and V.H. have nothing to declare.

References

1. **Laron Z, Pertzelan A, Mannheimer S** 1966 Genetic pituitary dwarfism with high serum concentation of growth hormone: a new inborn error of metabolism? Isr J Med Sci 2:152–155
2. **Rosenfeld RG, Rosenbloom AL, Guevara-Aguirre J** 1994 Growth hormone (GH) insensitivity due to primary GH receptor deficiency. Endocr Rev 15:369–390
3. **Rosenfeld RG, Hwa V** 2009 The growth hormone cascade and its role in mammalian growth. Horm Res 71:36–40
4. **Kofoed EM, Hwa V, Little B, Woods KA, Buckway CK, Tsubaki J, Pratt KL, Bezrodnik L, Jasper H, Tepper A, Heinrich JJ, Rosenfeld RG** 2003 Growth-hormone insensitivity (GHI) associated with a STAT-5b mutation. N Engl J Med 349:1139–1147
5. **Hwa V, Little B, Adiyaman P, Kofoed EM, Pratt KL, Ocal G, Berberoglu M, Rosenfeld RG** 2005 Severe growth hormone insensivity resulting from total absence of signal transducer and activator of transcription 5b. J Clin Endocrinol Metab 90:4260–4266
6. **Bernasconi A, Marino R, Ribas A, Rossi J, Ciaccio M, Oleastro M, Ornani A, Paz R, Rivarola MA, Zelazko M, Belgorosky A** 2006 Characterization of immunodeficiency in a patient with growth hormone insensitivity secondary to a novel STAT5b gene mutation. PEDIATRICS 118:e1584–e1592
7. **Vidarsdottir S, Walenkamp MJ, Pereira AM, Karperien M, van Doorn J, van Duyvenvoorde HA, White S, Breuning MH, Roelfsema F, Kruithof MF, van Dissel J, Janssen R, Wit JM, Romijn JA** 2006 Clinical and biochemical characteristics of a male patient with a novel homozygous STAT5b mutation. J Clin Endocrinol Metab 91: 3482–3485
8. **Hwa V, Camacho-Hübner C, Little BM, David A, Metherell LA, El-Khatib N, Savage MO, Rosenfeld RG** 2007 Growth hormone insensitivity and severe short stature in siblings: a novel mutation at the exon13-intron 13 junction of the STAT5b gene. Horm Res 68: 218–224
9. **Pugliese-Pires PN, Tonelli CA, Dora JM, Silva PC, Czepielewski M, Simoni G, Arnhold IJ, Jorge AA** 2010 A novel STAT5B mutation causing GH insenstivity syndrome associated with hyperprolactinemia and immune dysfunction in two male siblings. Eur J Endocrinol 163:349–355
10. **Cohen AC, Nadeau KC, Tu W, Hwa V, Dionis K, Bezrodnik L, Teper A, Gaillard M, Heinrich J, Krensky AM, Rosenfeld RG, Lewis DB** 2006 Cutting edge: decreased accumulation and regulatory function of $CD4^+CD25^{high}$ T cells in human STAT5b deficiency. J Immunol 177:2770–2774
11. **Lejarraga H, Orfila G** 1987 Estándares de peso y estatura para niños y niñas argentinos desde el nacimiento hasta la madurez. Arch Argent Pediatr 85:209–222
12. **Lejarraga H, Cusminsky M, Castro EP** 1976 Age of onset of puberty in urban argentinian children. Ann Hum Biol 3:379–381
13. **Lejarraga H, Sanchirico F, Cusminsky M** 1980 Age of Menarche in urban angentinian girls. Ann Hum Biol 7:579–581
14. **Martínez AS, Domené HM, Ropelato MG, Jasper HG, Pennisi PA, Escobar ME, Heinrich JJ** 2000 Estrogen priming effect on growth hormone (GH) provocative test: a useful tool for the diagnosis of GH deficiency. J Clin Endocrinol Metab 85:4168–4172
15. **Hattori N, Ikekubo K, Ishihara T, Moridera K, Hino M, Kurahachi H** 1994 Effects of anti-prolactin antoantibodies on serum prolactin measurements. Eur J Endocrinol 130:434–437
16. **Ballerini MG, Ropelato MG, Domené HM, Pennisi P, Heinrich JJ, Jasper HG** 2004 Differential impact of simple childhood obesity on the components of the growth hormone-insulin-like growth factor (IGF)-IGF binding proteins axis. J Pediatr Endocrinol Metab 17: 749–757
17. **Del Sal G, Manfioletti G, Schneider C** 1989 The CTAB-DNA precipitation method: a common mini-scale preparation of template DNA from phagemids, phages or plasmids suitable for sequencing. Biotechniques 7:514–520
18. **Hwa V, Little B, Kofoed EM, Rosenfeld RG** 2004 Transcriptional

regulation of insulin-like growth factor-I (IGF-I) by interferon-gamma (IFN-γ) requires Stat-5b. J Biol Chem 279:2728–2736
19. **Maamra M, Finidori J, Von Laue S, Simon S, Justice S, Webster J, Dower S, Ross R** 1999 Studies with a growth hormone antagonist and dual-fluorescent confocal microscopy demonstrate that the full-length human growth hormone receptor, but not the truncated isoform, is very rapidly internalized independent of JAK2-Stat5 signaling. J Biol Chem 274:14791–14798
20. **Fang P, Kofoed EM, Little BM, Wang X, Ross RJ, Frank SJ, Hwa V, Rosenfeld RG** 2006 A mutant signal transducer and activator of transcription 5B, associated with growth hormone insensitivity and insulin-like growth factor-I deficiency, cannot function as a signal transducer or transcription factor. J Clin Endocrinol Metab 91: 1526–1534
21. **Lappalainen I, Thusberg J, Shen B, Vihinen M** 2008 Genome wide analysis of pathogenic SH2 domain mutations. Proteins 72:779–792
22. **Kaneko T, Huang H, Zhao B, Li L, Liu H, Voss CK, Wu C, Schiller MR, Li SS** 2010 Loops govern SH2 domain specificity by controlling access to binding pockets. Sci Signal 3:ra34
23. **Chen X, Vinkemeier U, Zhao Y, Jeruzalmi D, Darnell Jr JE, Kuriyan J** 1998 Crystal Structure of a tyrosine phosphorylated STAT-1 dimer bound to DNA. Cell 93:827–839
24. **Becker S, Groner B, Müller CW** 1998 Three-dimensional structure of the STAT3β homodimer bound to DNA. Nature 394:145–151
25. **Kasembeli MM, Xu X, Tweardy DJ** 2009 SH2 domain binding to phosphopeptide ligands: potential for drug targeting. Front Biosci 14:1010–1022
26. **Mao X, Ren Z, Parker GN, Sondermann H, Pastorello MA, Wang W, McMurray JS, Demeler B, Darnell Jr JE, Chen X** 2005 Structural bases of unphosphorylated STAT1 association and receptor binding. Mol Cell 17:761–771
27. **Holland SM, DeLeo FR, Elloumi HZ, Hsu AP, Uzel G, Brodsky N, Freeman AF, Demidowich A, Davis J, Turner ML, Anderson VL, Darnell DN, Welch PA, Kuhns DB, Frucht DM, Malech HL, Gallin JI, Kobayashi SD, Whitney AR, Voyich JM, Musser JM, Woellner C, Schäffer AA, Puck JM, Grimbacher B** 2007 STAT3 mutations in the hyper-IgE syndrome. N Engl J Med 357:1608–1619
28. **Renner ED, Torgerson TR, Rylaarsdam S, Añover-Sombke S, Golob K, LaFlam T, Zhu Q, Ochs HD** 2007 STAT3 mutation in the original patient with Job's syndrome. N Eng J Med 357:1667–1668
29. **Derr MA, Fang P, Sinha SK, Ten S, Hwa V, Rosenfeld RG** 2011 A novel Y332C missense mutation in the intracellular domain of the human growth hormone receptor (GHR) does not alter STAT5b signaling: redundancy of GHR intracellular tyrosines involved in STAT5b signaling. Horm Res Paediatr 75:187–199
30. **Woldman I, Varinou L, Ramsauer K, Rapp B, Decker T** 2001 The Stat1 binding motif of the interferon-γ receptor is sufficient to mediate Stat5 activation and its repression by SOCS3. J Biol Chem 276:45722–45728
31. **Hwa V, Nadeau K, Wit JM, Rosenfeld RG** 2011 STAT5b deficiency: lessons from STAT5b gene mutations. Best Pract Res Clin Endocrinol Metab 25:61–75
32. **Aynsley-Green A, Zachmann M, Prader A** 1976 Interrelation of the therapeutic effects of growth hormone and testosterone on growth in hypopituitarism. J Pediatr 89:992–999
33. **Walenkamp MJ, Vidarsdottir S, Pereira AM, Karperien M, van Doorn J, van Duyvenvoorde HA, Breuning MH, Roelfsema F, Kruithof MF, van Dissel J, Janssen R, Wit JM, Romijn JA** 2007 Growth hormone secretion and immunological function of a male patient with a homozygous STAT5b mutation. Eur J Endocrinol 156:155–165